



Title	Sensitivity of the neutron multiplication factor to gadolinium isotopes' nuclear data for light water reactor fuel assemblies in the peak reactivity burnup range
Author(s)	Chiba, Go
Citation	Annals of nuclear energy, 151, 107949 https://doi.org/10.1016/j.anucene.2020.107949
Issue Date	2021-02
Doc URL	https://hdl.handle.net/2115/87074
Rights	© 2021. This manuscript version is made available under the CC-BY-NC-ND 4.0 license http://creativecommons.org/licenses/by-nc-nd/4.0/
Rights(URL)	https://creativecommons.org/licenses/by-nc-nd/4.0/
Type	journal article
File Information	main_r2.pdf



Sensitivity of the neutron multiplication factor to gadolinium isotopes' nuclear data for light water reactor fuel assemblies in the peak reactivity burnup range

Go Chiba^{*,a}

^a*Hokkaido University, Kita-ku, Sapporo, Hokkaido 060-8628, Japan*

Abstract

The reactivity of a fuel assembly including burnable absorbers can become the largest at low fuel burnup, so the accuracy of reactivity calculations for such systems is important. To investigate this issue, the impact of gadolinium isotopes' nuclear data on neutron multiplication factor k is quantified. Sensitivities of k to nuclear data are calculated from 0 to 20 GWD/t for a BWR 3×3 multicell model. Sensitivity to gadolinium-157 (n, γ) cross section becomes the largest at the zero burnup. Sensitivity to gadolinium-155 (n, γ) cross sections takes the two largest values and the second one is observed around fuel burnup where the reactivity reaches its peak. Sensitivities are also calculated for BWR and PWR assemblies, and similar trends are observed. Finally, nuclear data-induced uncertainties of k are quantified. Gadolinium-157 contribution is the largest at zero burnup, and gadolinium-155 contribution is relatively important around fuel burnup corresponding to the reactivity peak.

Key words: Burnable absorber, gadolinium, depletion perturbation theory, uncertainty quantification

1. Introduction

The use of burnable absorbers in nuclear fuels to suppress the excess reactivity at the beginning of nuclear reactor operations has been quite a familiar concept in thermal reactors, and generally gadolinium-oxide (or gadolinia) is used by mixing it with uranium-dioxide. There are six stable gadolinium isotopes, and it is well known that gadolinium-155 and -157 have significantly large (n, γ) cross sections, especially for thermal neutrons. By adopting these burnable absorbers, the neutron multiplication factor at the beginning of reactor operation is dramatically reduced, so the initial excess reactivity can be suppressed and the reactivity management becomes relatively easy. With reactor operation, these burnable absorbers are depleted, and other gadolinium isotopes with low (n, γ) cross sections are generated. Thus the neutron multiplication factor increases until, after a certain burnup period, most of nuclides initially present in the

*Corresponding author, Tel: +81-10-706-6683, Fax: +81-10-706-6683

Email address: go_chiba@eng.hokudai.ac.jp (Go Chiba)

Preprint submitted to Elsevier

January 27, 2021

11 burnable absorbers have been depleted and converted to other nuclides, so the multiplication factor begins
12 to decrease with burnup as in nuclear fuels without burnable absorbers. This means that there should be a
13 peak of reactivity during fuel burnup in nuclear fuels with burnable absorbers. Generally, nuclear fuels are
14 burned in a nuclear reactor core until they reach on average around 35 GWD/t burnup at discharge, but due
15 to various reasons, there is a possibility that irradiated nuclear fuels with low fuel burnup are also treated
16 outside of a reactor core, such as in a water pool. For a water pool containing irradiated nuclear fuels,
17 proper criticality management should be conducted; reactivity of a system should be accurately estimated
18 and sub-criticality of this system should be assured. Reactivity prediction generally relies on numerical
19 simulation, and the fact that the largest reactivity can be found not in fresh fuel but in low-burnup fuel if
20 nuclear fuel in this system includes burnable absorbers should be carefully considered. This suggests that
21 numerical prediction of the neutron multiplication factor around fuel burnup corresponding to full depletion
22 of burnable absorbers is important.

23 The numerical prediction of the evolution of the neutron multiplication factor of a system along burnup
24 should include various types of uncertainties, one of them being the uncertainty induced by nuclear data
25 which are used in nuclear fuel burnup calculations and reactivity calculations of neutron multiplying systems.
26 It is needless to say that nuclear data of major actinides such as uranium and plutonium are important,
27 but nuclear data of other nuclides including burnable absorbers (i.e., gadolinium isotopes) should also be
28 considered for the above-mentioned reasons.

29 To quantify nuclear data-induced uncertainty of neutron multiplication factor during nuclear fuel bur-
30 nup, the Monte Carlo sampling procedure based on a number of calculation cases with randomly-sampled
31 nuclear data has been widely used in the field of reactor physics, and a lot of works and results have been
32 accumulated(Rochman, 2012, 2014; Yamamoto, 2015; Leray, 2017). However, as far as the authors know,
33 no such studies focusing on the neutron multiplication factor around full depletion of burnable absorbers
34 have been published so far.

35 The present work addresses nuclear data-induced uncertainties of the neutron multiplication factor
36 around full depletion of burnable absorbers in light water reactor (LWR) fuel assemblies. Uncertainty
37 quantification will be carried out not with the Monte Carlo sampling procedure but with a sensitivity-based
38 approach; sensitivities of the neutron multiplication factor with respect to nuclear data are initially cal-
39 culated, and then nuclear data-induced uncertainties are quantified with these sensitivities and covariance
40 data of nuclear data. The capability to calculate sensitivities of reactor physics parameters to nuclear data
41 during nuclear fuel burnup in LWR fuel assemblies including burnable absorbers has been recently devel-
42 oped(Chiba, 2016a, 2018a), based on the generalized perturbation theory for spatially-dependent nuclear fuel
43 depletion problems, the *depletion perturbation theory* (DPT), established by Gandini(Gandini, 1969) and
44 Williams(Williams, 1979). With this new capability, sensitivities can be easily calculated. Another merit
45 of this approach is that it can help understand how nuclear data affects calculation results, i.e., neutron

46 multiplication factor change during fuel burnup.

47 When conducting nuclear data-induced uncertainty quantification, reliable covariance data are manda-
48 tory. Among the widely-used evaluated nuclear data libraries, ENDF/B, JEFF and JENDL, the ENDF/B
49 and JEFF libraries provide covariance data for gadolinium isotopes. However, the latest version of these
50 libraries, ENDF/B-VIII.0 and JEFF-3.3, adopt the identical data obtained in 2009 through the international
51 collaboration in the framework of the Working Party of International Evaluation Co-operation of the Nu-
52 clear Energy Agency within the Organisation for Economic Co-operation and Development(NEA, 2009). In
53 the present work, these covariance data will be used, however it is important to underline that uncertainty
54 quantification analyses are highly dependent on the covariance data used. For this reason, the analyses will
55 be focused on the sensitivities.

56 The present paper is organized as follows. Section 2 describes basic data, theory and procedure about
57 sensitivity analyses and uncertainty quantification for the neutron multiplication factor during nuclear fuel
58 burnup. Section 3 presents problem specifications for nuclear fuel burnup and all the numerical results, and
59 the conclusion is given in Section 4.

60 **2. Data, theory and procedure of sensitivity analyses and uncertainty quantification**

61 *2.1. Nuclear data and their covariance data*

62 In the present work, sensitivities are calculated with the JENDL library: JENDL-4.0(Shibata, 2011)
63 for neutron-induced reaction cross sections, JENDL/FPY-2011 and JENDL/FPD-2011(Katakura, 2011) for
64 fission yield data and decay data of fission products (FP). Calculated sensitivities are used to quantify
65 nuclear data-induced uncertainties of the neutron multiplication factor. The present work mainly focuses
66 on gadolinium isotopes' nuclear data, but to assess the impact of gadolinium nuclear data uncertainty
67 in the total uncertainty, uncertainties of reaction cross sections of major actinides, fission yields, decay
68 constants and decay branching ratios are also taken into account. Generally, uncertainty information on
69 these nuclear data are provided as covariance data in evaluated nuclear data libraries. In JENDL-4.0,
70 covariance data are evaluated for almost all the important actinides, and those are taken into account in
71 the present study. However, as mentioned in the introduction, JENDL-4.0 provides no covariance data for
72 reaction cross sections of gadolinium isotopes, so we will use covariance data for these nuclear data taken
73 from ENDF/B-VIII.0(Brown, 2018). In JENDL/FPY-2011, fission yield data are given to 1,299 FP. Only
74 variance data are provided to fission yield data in JENDL/FPY-2011 due to the format limitation, but it
75 has been pointed out by many authors that correlations in fission yield data among different nuclides should
76 be taken into account to properly conduct uncertainty propagation calculations(Katakura, 2011; Fiorito,
77 2016). While there have been several methods to consider correlations, we will adopt the generalized
78 least-square (GLS) updating procedure which introduces information about chain yields and some physical

79 constraints about fission reactions(Fiorito, 2016). On the decay branching ratio, correlations due to the
80 physical constraints (the normalization condition) are taken into account.

81 2.2. Sensitivity calculations with the depletion perturbation theory

For a certain nuclide, the relative sensitivity of neutron multiplication factor k to nuclear data σ_i is defined as

$$s_i = \frac{dk}{d\sigma_i} \cdot \frac{\sigma_i}{k}. \quad (1)$$

82 Since quite a large number of nuclear data are used in nuclear fuel burnup calculations, numerical
83 differentiation to obtain s_i is unrealistic. Therefore, DPT will be used to calculate sensitivities of k during
84 nuclear fuel burnup with respect to nuclear data such as neutron-induced reaction cross sections, fission
85 yields, decay constants and decay branching ratios. Details about DPT can be found in references(Gandini,
86 1969; Williams, 1979).

87 Numerical calculations of sensitivities with DPT are generally based on numerical methods for nuclear
88 fuel burnup calculations, which consist of neutron flux distribution calculations by solving the neutron
89 transport equation and nuclides transmutation calculations. In the present study, all these calculations are
90 carried out with a reactor physics code system CBZ(Chiba, 2019) which has been developed at Hokkaido
91 University.

92 In nuclear fuel burnup calculations, generation and transmutation of FP should be numerically simulated.
93 Since there are a large number of FP, over 1,000, it is computationally expensive to treat all these FP
94 explicitly in nuclide transmutation calculations, especially in a complicated system like LWR fuel assemblies.
95 Furthermore, the computational burden increases even more when the DPT calculations are carried out since
96 a huge amount of data during nuclear fuel burnup should be stored in computer memory. In order to solve
97 these problems, a simplified nuclide chain model is used consisting of 138 FP(Chiba, 2015) with which
98 reactivity during fuel burnup can be accurately calculated.

99 For resonance calculations, the advanced Bondarenko method(Chiba, 2016b) is adopted, and medium-
100 wise 107-group cross section data are generated. Energy structure of the 107-group is that of the SRAC
101 code developed for thermal reactor analyses(Okumura, 2006). Background cross sections required in the
102 advanced Bondarenko method are calculated from the Dancoff factors evaluated with a whole assembly
103 model(Sugimura, 2006). Neutron transport calculations with the 107-group cross sections including gener-
104 alized adjoint neutron flux calculations for DPT are performed with a neutron transport calculation module
105 MEC(van Rooijen, 2011) based on the method of characteristics, and reaction rates are calculated for all
106 the media containing nuclear fuels. Note that angular integration of bilinear functions of neutron flux and
107 generalized adjoint neutron flux in DPT should be carefully carried out in a system including strong neutron
108 absorbers(Chiba, 2018a). Scattering anisotropy is taken into account by the P0 transport approximation.

109 Nuclides transmutation calculations are carried out with the simplified nuclide chain model as mentioned
 110 above. Nuclides transmutation equations including adjoint problems in DPT are solved by the matrix
 111 exponential method with the mini-max polynomial approximation method(Kawamoto, 2015). To reduce
 112 the time-discretization error, the predictor-corrector method is employed.

The relative sensitivity of k at fuel burnup t to σ can be calculated as follows:

$$\frac{dk}{d\sigma} \cdot \frac{\sigma}{k} = \left\{ \frac{\partial k}{\partial \sigma} + \frac{\partial k}{\partial \Phi(t)} \cdot \frac{d\Phi(t)}{d\sigma} + \frac{\partial k}{\partial \mathbf{N}(t)} \cdot \frac{d\mathbf{N}(t)}{d\sigma} \right\} \cdot \frac{\sigma}{k}, \quad (2)$$

113 where $\Phi(t)$ and $\mathbf{N}(t)$ are vectors representing neutron flux and nuclides number density at t . The first and
 114 second terms in the parenthesis of right-hand-side of this equation can be easily calculated with the classical
 115 perturbation theory, and are referred to as *static component*. On the other hand, the third term can be
 116 calculated with the classical perturbation theory and DPT, and is referred to as *burnup component*(Chiba,
 117 2016a).

118 2.3. Uncertainty quantification with sensitivities and covariance data

Nuclear data-induced uncertainties of k can be easily quantified if sensitivities of k with respect to nuclear
 data are available. The relative uncertainty in k due to nuclear data can be calculated with the following
 equation:

$$\Delta k/k = \sqrt{\sum_i \sum_{i'} s_i s_{i'} \text{cov}(\sigma_i, \sigma_{i'})}, \quad (3)$$

where $\text{cov}(\sigma_i, \sigma_{i'})$ is a relative covariance between σ_i and $\sigma_{i'}$, and a covariance matrix covering all the nuclear
 data considered is defined as \mathbf{V}_σ here. When we define a sensitivity vector \mathbf{s} as $\mathbf{s} = (s_1 \ s_2 \ \cdots \ s_I)^T$, where
 T is for vector transposition, $\Delta k/k$ can be rewritten using \mathbf{V}_σ and \mathbf{s} as

$$\Delta k/k = \sqrt{\mathbf{s}^T \mathbf{V}_\sigma \mathbf{s}}. \quad (4)$$

119 Since a simplified nuclide chain model is used, sensitivities of k to nuclear data are calculated within
 120 the framework of this simplified model, so in the uncertainty quantification calculations, covariance data
 121 consistent with the simplified chain model should be used. Discussion about this issue, as well as the
 122 numerical method and tool developed, can be found in reference(Chiba, 2018b) and will be used in the
 123 following.

124 3. Numerical tests and results

125 3.1. Problem specifications

126 Sensitivities of k with respect to nuclear data including (n, γ) cross sections of gadolinium isotopes during
 127 nuclear fuel burnup are calculated with high resolution (per 0.1 GWD/t) for a 3×3 multicell model. In this
 128 model, a gadolinium-bearing fuel pin is loaded at the center position and it is surrounded by uranium fuel

129 pins whose uranium-235 enrichment is 3.9 wt%. Geometrical and material specifications are taken from a
130 BWR fuel assembly model developed through the OECD/NEA burnup credit benchmark phase-IIIC(NEA,
131 2015). Reflective boundary conditions are adopted. The geometrical specification of the 3×3 multicell
132 model and the original BWR assembly model is shown in **Fig. 1**. As for coolant condition, two different
133 void fractions of 0% and 40% are considered. The infinite neutron multiplication factor during fuel burnup
134 of this 3×3 multicell model is shown in **Fig. 2**. The reactivity peaks are observed at around 13 GWD/t. In
135 the original BWR fuel assembly model, a square-shaped large water channel is located inside the assembly,
136 so neutron moderation by water in this 3×3 model is less enhanced than the original assembly model. With
137 the calculated sensitivities and nuclear data covariance matrix, nuclear data-induced uncertainties of k can
138 be also quantified with high resolution for fuel burnup.

139 In addition to the 3×3 multicell model, sensitivities of k with respect to (n,γ) cross sections of gadolinium
140 isotopes are calculated for the original BWR assembly with three different void conditions (0%, 40% and
141 70%) and two PWR assemblies prepared in the VERA depletion benchmark suite(Kim, 2015) with low
142 resolution (per 1.0 GWD/t). The geometrical specification of these PWR assembly models, 2O and 2P, is
143 shown in **Fig. 3**. Weight percent of Gd_2O_3 in gadolinium-bearing fuel rods is 5.0% in both the BWR and
144 PWR assemblies. The infinite neutron multiplication factor of these BWR and PWR assemblies with fuel
145 burnup is shown in **Figs. 4** and **5**, respectively. As shown in these figures, fuel burnup where full depletion
146 of gadolinium isotopes is attained is different from each other: the gadolinium isotopes burn out earlier
147 in the PWR assemblies (around 8 GWD/t) than in the BWR assembly (around 12 GWD/t) because of a
148 difference in fuel pin diameter.

149 *3.2. Detailed sensitivity profiles of k to (n,γ) cross sections of gadolinium isotopes in the 3×3 multicell* 150 *model*

151 In this section, sensitivities of k to (n,γ) cross section of gadolinium isotopes in the 3×3 multicell model
152 from 0 to 20 GWD/t are presented.

153 The k sensitivities can be calculated to every group cross section, and sensitivities to one-group (energy-
154 averaged) cross section can be easily calculated by summing up all these sensitivities. One-group sensitivity
155 is a useful quantity since it can be used to estimate the impact on k of average change in the cross section.
156 Sensitivities of k to one-group (n,γ) cross section of gadolinium isotopes are shown in **Figs. 6** to **9**. In
157 addition to total sensitivities, static and burnup components are also presented.

158 Among all the isotopes and during the whole fuel burnup period, maximum sensitivity is observed in
159 gadolinium-157 cross section at zero fuel burnup.

160 Regarding gadolinium-155 and -157, which are strong neutron absorbing isotopes, large negative static
161 components are observed at the beginning of fuel burnup. The gadolinium-157 static component becomes
162 small with fuel burnup because of their depletion. The gadolinium-155 static component increases with

163 fuel burnup at the beginning, and begins to decrease around 4 GWD/t. The static components of energy-
 164 dependent sensitivity to gadolinium-155 (n,γ) cross section at the 0% void condition are shown in **Fig. 10**.
 165 Since (n,γ) cross section of gadolinium-157 is larger than that of gadolinium-155, gadolinium-157 is depleted
 166 quickly at the beginning of fuel burnup, and shifting of the neutron flux or neutron spectrum to lower energies
 167 is expected. The (n,γ) cross section of gadolinium-155 is large in low energy range, so this neutron flux
 168 energy spectra shifting enhances neutron capture of gadolinium-155 with fuel burnup. Burnup components
 169 of sensitivities to gadolinium-155 and -157 increase from zero with fuel burnup in the low burnup range. Let
 170 us consider k at certain fuel burnup. If (n,γ) cross section of these isotopes is increased, neutron absorption
 171 rate at this fuel burnup should be increased, but the depletion of these isotopes becomes fast and number
 172 densities of these isotopes at this fuel burnup should be small. The former and latter correspond to the
 173 static and burnup components, respectively, and the cancellation between these two components can be
 174 expected. As a result of this cancellation, there exists fuel burnup where the total sensitivity becomes zero.
 175 After full depletion of gadolinium-155 and -157, the total sensitivities of these isotopes become close to zero.
 176 On gadolinium-157, total sensitivity takes its maximum at zero fuel burnup because of large contribution of
 177 the static component. On the other hand, on gadolinium-155, two peaks can be found around fuel burnup
 178 of 2 GWD/t and at 11 GWD/t in the 0% void fraction case and at 14 GWD/t in the 40% void fraction
 179 case. This is because (n,γ) cross section of gadolinium-155 is smaller than that of gadolinium-157 and the
 180 gadolinium-155 depletion should follow the depletion of gadolinium-157.

181 Regarding gadolinium-154 and -156, which can be converted to gadolinium-155 and -157 via (n,γ) re-
 182 action, both the components are negative and the burnup component becomes large with fuel burnup by
 183 the burnup of 10 GWD/t. Thus the total sensitivities also become large with fuel burnup in this burnup
 184 range. The reason why the burnup component is negative is that (n,γ) reaction of these isotopes generate
 185 more neutron absorbing isotopes: gadolinium-155 and -157. The total sensitivity of gadolinium-156 is larger
 186 than that of gadolinium-154. After fuel burnup corresponding to full depletion of gadolinium-155 and -157,
 187 the burnup components tend to decrease with fuel burnup, and this decrease in gadolinium-154 is more
 188 significant than in gadolinium-156 since gadolinium-154 has no parent nuclide in a nuclide chain.

189 Energy-dependent sensitivities of k at 0.1 GWD/t and 12 GWD/t (or 10 GWD/t) in void fraction of
 190 0% are shown in **Fig. 11**. Sensitive energy ranges of each isotope can be specified from these figures.
 191 Contributions of sensitivities in thermal neutron energy range are dominant in gadolinium-155 and -157.
 192 In gadolinium-154, contributions of epi-thermal neutron energy range are comparable with contributions of
 193 thermal energy range, and in gadolinium-156 contribution of epi-thermal neutron energy range is dominant.
 194 Energy-dependent sensitivities in void fraction of 40% are also shown in **Fig. 12**.

195 *3.3. Sensitivity profiles of k to (n,γ) cross sections of gadolinium isotopes in the BWR and PWR assemblies*

196 In the preceding section, component-wise sensitivities of k to (n,γ) cross sections of gadolinium isotopes
197 have been carefully examined with high resolution for fuel burnup, and energy-dependent sensitivities have
198 been also presented in the 3×3 multicell model. In order to obtain more general conclusions, sensitivities
199 for the BWR and PWR assemblies with lower resolution for fuel burnup are calculated

200 Total sensitivities of the BWR assembly with different void conditions are shown in **Fig. 13**. Since
201 the BWR assembly includes the central water channel and the water gap channel outside the channel box,
202 neutron moderation is enhanced in comparison with the 3×3 multicell model. As the result, absolute values
203 of sensitivities to (n,γ) cross sections of gadolinium-154, -155 and -157, in which contribution of thermal
204 neutron energy range is dominant as shown in Fig. 11, becomes larger than those of the 3×3 multicell model
205 by less than a factor of 2. Dependence on void fractions and on fuel burnup is quite similar with the 3×3
206 multicell model. Sensitivities to gadolinium-156 in the BWR assembly is generally smaller than those in the
207 3×3 multicell model, but the difference is not significant.

208 Total sensitivities of the PWR assemblies are shown in **Fig. 14**. Since gadolinium isotopes in these PWR
209 assemblies burn out earlier than in the BWR 3×3 multicell model, dependence of sensitivities on fuel burnup
210 is slightly different from that in the 3×3 model, but the trend is similar. Absolute values of sensitivities of
211 gadolinium-155 and -157 in 2P are comparable with those in the BWR 3×3 multicell model and the BWR
212 assembly, and absolute values of sensitivities of the other gadolinium isotopes are generally smaller than
213 those in the BWR problems.

214 From these results, we have confirmed that trends in sensitivities of k to (n,γ) cross sections of gadolinium
215 isotopes are very similar among the BWR 3×3 multicell model, the BWR assembly and the PWR assemblies.

216 *3.4. Uncertainty quantification in k due to neutron-induced nuclear data for the 3×3 multicell model*

217 To assess the impact of the (n,γ) cross section uncertainties of gadolinium isotopes in k , uncertainty
218 propagation calculations are performed for the BWR 3×3 multicell model with sensitivities calculated in
219 the preceding section.

220 As mentioned above, ENDF/B-VIII.0 is the reference for the uncertainty of (n,γ) cross sections of
221 gadolinium isotopes. Relative standard deviations of 107-group (n,γ) cross sections of gadolinium isotopes,
222 obtained from the evaluated data in ENDF/B-VIII.0, are shown in **Fig. 15**, and correlation matrices among
223 different energy groups for each isotope are shown in **Fig. 16**.

224 With covariance data of nuclear data including (n,γ) cross sections of gadolinium isotopes, uncertainty
225 of k is quantified as shown in **Fig. 17**. Uncertainty is the largest at zero fuel burnup, and becomes almost
226 constant after around 5 GWD/t. In the result of the void condition of 40%, a small local peak is observed
227 at around 12 GWD/t. Component-wise uncertainty of k is shown in **Fig. 18**, and it can be found that
228 neutron-induced reaction cross section uncertainties are dominant in the k uncertainties. This result is

229 consistent with the previous works if fission yield covariance data are generated with the GLS (or GLS-
 230 like) method(Leray, 2017; Chiba, 2018b). **Figure 19** shows reaction cross section-induced uncertainties of
 231 k decomposed into heavy metal (HM) components and gadolinium isotopes (Gd) components. Based on
 232 covariance data of heavy metal nuclides from JENDL-4.0 and those of gadolinium isotopes from ENDF/B-
 233 VIII.0, uncertainty induced by nuclear data of heavy metal nuclides is dominant in the k uncertainties.
 234 In the gadolinium nuclear data-induced uncertainties, the largest value is observed at zero fuel burnup and
 235 small local peaks can be observed at around 12 GWD/t. Gadolinium isotope-wise k uncertainties induced by
 236 (n,γ) cross sections are shown in **Fig. 20**. Contribution of gadolinium-157 is dominant when the fuel is fresh,
 237 and it decreases with fuel burnup by 6 GWD/t. Around 10 GWD/t, there is a peak in the gadolinium-
 238 157 contribution, but the height of this peak is much lower than that at zero fuel burnup. This can be
 239 understood by seeing sensitivities shown in Fig. 9. In gadolinium-155-induced uncertainties, two peaks can
 240 be observed around 2 GWD/t and 12 GWD/t in the 0% void fraction case and 0 GWD/t and 14 GWD/t
 241 in the 40% void fraction case, and heights of these two peaks are comparabale with each other as expected
 242 from sensitivities shown in Fig. 7. This second peak contributes to a small local peak observed in the k
 243 uncertainties shown in Fig. 17. Fuel burnup where this second peak is observed corresponds to that of full
 244 depletion of gadolinium isotopes and that where k takes the largest value during fuel burnup. This result
 245 suggests that gadolinium-155 nuclear data is more important than gadolinium-157 nuclear data from a view
 246 point of reactivity management of irradiated nuclear fuel with low fuel burnup. It is also interesting to
 247 point out that gadolinium-156 contribution is not negligible because of ralatively large standard deviation
 248 of around 15% and large positive correlation in sensitive energy ranges from 1 eV to 1 keV evaluated in
 249 ENDF/B-VIII.0.

250 4. Conclusion

251 The reactivity (or neutron multiplication factor) of a fuel assembly including burnable absorbers can
 252 become the largest not at zero fuel burnup but at low fuel burnup, so the accuracy of reactivity calculations
 253 for such systems at low fuel burnup is important. In order to investigate this issue, the impact of gadolinium
 254 isotopes' nuclear data of on k has been quantified.

255 Sensitivities of k with respect to various nuclear data including neutron-induced reaction cross sections
 256 of gadolinium isotopes have been calculated with the CBZ code system, in which a capability based on
 257 the depletion perturbation theory has been implemented. Total and component-wise sensitivities of k to
 258 (n,γ) cross sections of gadolinium isotopes have been calculated with high resolution for fuel burnup for
 259 the BWR 3×3 multicell model, and physical interpretations have been provided. From the observations of
 260 the sensitivities, the following have been obtained: (1) sensitivity to gadolinium-157 cross section becomes
 261 the largest at zero burnup, and (2) sensitivity to gadolinium-155 cross sections takes the two largest values

262 during fuel burnup and the second one is observed at fuel burnup where reactivity peak is observed. The
263 burnup where the largest sensitivity values are observed are dependent on the void fraction; 2 GWD/t
264 and 11 GWD/t in the 0% void fraction case and 2 GWD/t and 14 GWD/t in the 40% void fraction case.
265 Energy-dependent sensitivities have been also provided.

266 In order to obtain more general conclusions, sensitivities of k to (n,γ) cross sections of gadolinium isotopes
267 have been calculated for the BWR and PWR assemblies, and it has been confirmed that the trend observed
268 in the BWR 3×3 multicell model also appears in these assemblies.

269 Finally, with the sensitivities calculated with the depletion perturbation theory, nuclear data-induced un-
270 certainties of k have been quantified. In this calculation, covariance data given in JENDL-4.0 and ENDF/B-
271 VIII.0 have been used for cross sections, and those given in JENDL/FPY-2011 and JENDL/FPD-2011 have
272 been used for fission yield and decay-relevant data. Among these nuclear data, cross sections of heavy metal
273 nuclides are dominant contributors to total k uncertainties. On k uncertainties induced by gadolinium
274 isotopes' nuclear data, gadolinium-157 contribution is the largest at zero fuel burnup, but gadolinium-155
275 contribution is relatively important around fuel burnup of 13 GWD/t where k takes the largest value during
276 fuel burnup.

277 Based on the above results, it can be concluded that uncertainties of k induced by gadolinium isotopes
278 nuclear data are not significant during nuclear fuel burnup. This conclusion deserves a careful consideration,
279 since uncertainty quantification analyses are strongly dependent on the input covariance data and evaluators
280 and new state-of-the-art covariance matrices are released, it is strongly recommended that the impact of
281 gadolinium nuclear data uncertainties on k during burnup is once again examined.

282 Acknowledgements

283 This work is motivated by a suggestion from Dr. Toshihisa Yamamoto and Dr. Tatsuya Fujita of The
284 Secretariat of the Nuclear Regulation Authority (S/NRA) in Japan.

285 References

- 286 Brown, D.A., et al., 2018. ENDF/B-VIII.0: The 8th major release of the nuclear reaction data library with CIELO-project
287 cross sections, new standards and thermal scattering data, Nucl. Data Sheets, 148, 1-142.
- 288 Chiba, G., et al., 2015. Important fission product nuclides identification method for simplified burnup chain construction, J.
289 Nucl. Sci. Technol., 52, 953-960.
- 290 Chiba, G., et al., 2016. Development of a fuel depletion sensitivity calculation module for multicell models in a deterministic
291 reactor physics code CBZ. Ann. Nucl. Energy, 96, 313-323.
- 292 Chiba, G., et al., 2016. Advanced Bondarenko method for resonance self-shielding calculations in deterministic reactor physics
293 code system CBZ, Ann. Nucl. Energy, 96, 277-286.
- 294 Chiba, G., 2018a. Perturbation theory for nuclear fuel depletion calculations with predictor-corrector method. J. Nucl. Sci.
295 Technol., 55. 290-300.

296 Chiba, G., Okumura, S., 2018b. Uncertainty quantification of neutron multiplication factors of light water reactor fuels during
297 depletion. *J. Nucl. Sci. Technol.*, 55, 1043-1053.

298 Chiba, G., Endo, T., 2019. Numerical benchmark problem of solid-moderated enriched-uranium-loaded core at Kyoto university
299 critical assembly, *J. Nucl. Sci. Technol.*, 57, 187-195.

300 Fiorito, L., et al., 2016. Generation of fission yield covariances to correct discrepancies in the nuclear data libraries, *Ann. Nucl.*
301 *Energy*, 88, 12-23.

302 Gandini, A., 1969. A method of correlation of burnup measurements for physics prediction of fast power-reactor life. *Nucl. Sci.*
303 *Eng.*, 38, 1-7.

304 Katakura, J., 2011. JENDL FP decay data file 2011 and fission yields data file 2011, JAEA-Data/Code 2011-025, Japan Atomic
305 Energy Agency.

306 Kawamoto, Y., Chiba, G., Tsuji, M., et al. 2015. Numerical solution of matrix exponential in burn-up equation using mini-max
307 polynomial approximation, *J. Nucl. Sci. Technol.*, 80, 219-224.

308 Kim, K.S., 2015. Specification for the VERA depletion benchmark suite, CASL-U-2015-PHI.CVS.P11.02-010, Oak Ridge
309 National Laboratory.

310 Leray, O., et al., 2017. Uncertainty propagation of fission product yields to nuclide composition and decay heat for a PWR
311 UO₂ fuel assembly. *Prog. Nucl. Energy*, 101, 486-495.

312 Nuclear Energy Agency (NEA), 2009. Evaluated data library for the bulk of fission products, Vol. 23, International Evalua-
313 tion Co-operation, A report by the Working Party on International Evaluation Co-operation of the NEA Nuclear Science
314 Committee, NEA/WPEC-23, OECD/NEA, Paris.

315 Nuclear Energy Agency (NEA), 2015. Burn-up credit criticality safety benchmark phase III-C. NEA/NSC/R/(2015)6,
316 OECD/NEA, Paris.

317 Okumura, K., et al., 2006. SRAC2006: a comprehensive neutronics calculation code system, JAEA-Data/Code 2007-004, Japan
318 Atomic Energy Agency.

319 Rochman, D., et al., 2012. Propagation of ^{235,236,238}U and ²³⁹Pu nuclear data uncertainties for typical PWR fuel element.
320 *Nucl. Technol.*, 179, 323-338.

321 Rochman, D., et al., 2014. Efficient use of Monte Carlo: uncertainty propagation. *Nucl. Sci. Eng.*, 177, 337-349.

322 van Rooijen, W.F.G., Chiba, G., 2011. Diffusion coefficient for LMFBR cells calculated with MOC and Monte Carlo methods.
323 *Ann. Nucl. Energy*, 38, 133-144.

324 Shibata, K., et al., 2011. JENDL-4.0: a new library for nuclear science and engineering, *J. Nucl. Sci. Technol.*, 48, 1-30.

325 Sugimura, N., Yamamoto, A., 2006. Evaluation of Dancoff factors in complicated geometry using the method of characteristics,
326 *J. Nucl. Sci. Technol.*, 43, 1182-1187.

327 Williams, M.L., 1979. Development of depletion perturbation theory for coupled neutron/nuclide fields. *Nucl. Sci. Eng.*, 70,
328 20-36.

329 Yamamoto, A., et al., 2015. Uncertainty quantification of LWR core characteristics using random sampling method. *Nucl. Sci.*
330 *Eng.*, 181, 160-174.

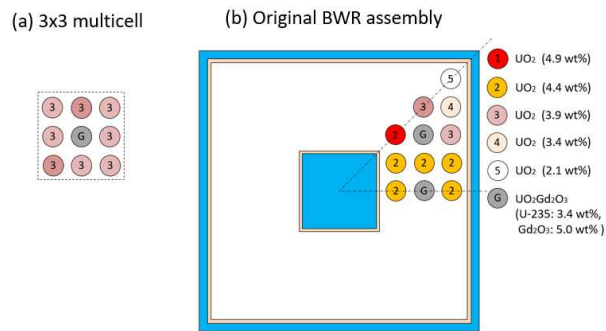


Figure 1: Geometrical specification of the 3×3 multicell model and the BWR assembly model

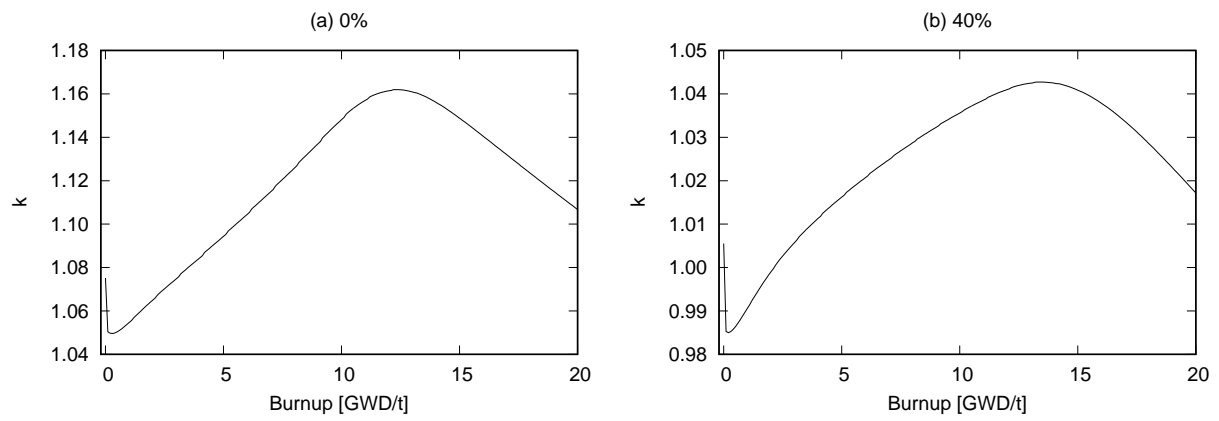


Figure 2: Infinite neutron multiplication factor of the 3×3 multicell model during nuclear fuel burnup

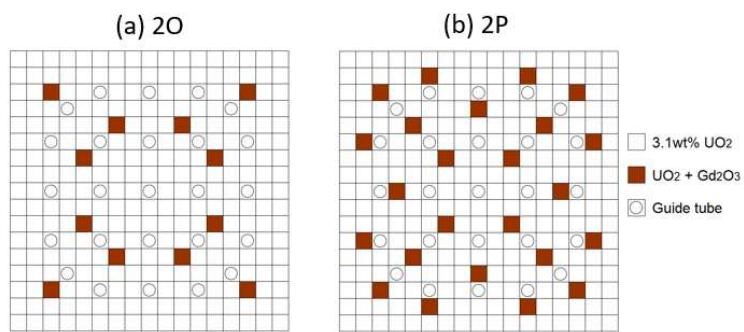


Figure 3: Geometrical specification of the PWR assembly models in the VERA depletion benchmark suite

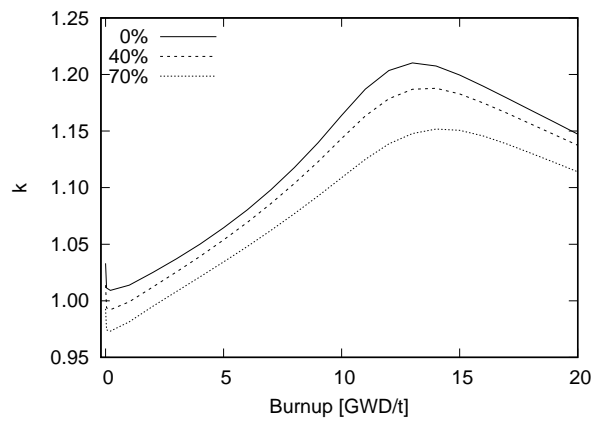


Figure 4: Infinite neutron multiplication factor of the BWR assembly with different void fraction

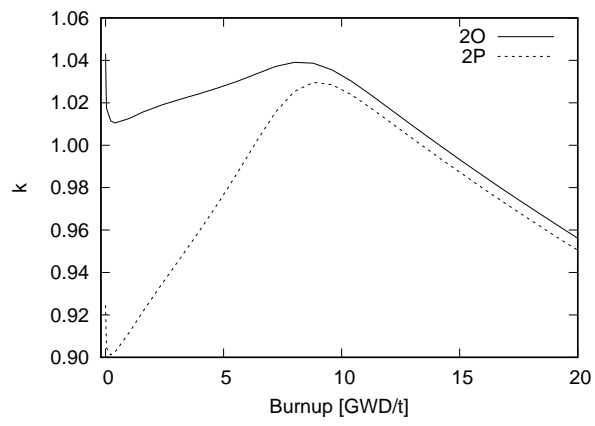


Figure 5: Infinite neutron multiplication factor of the PWR assemblies

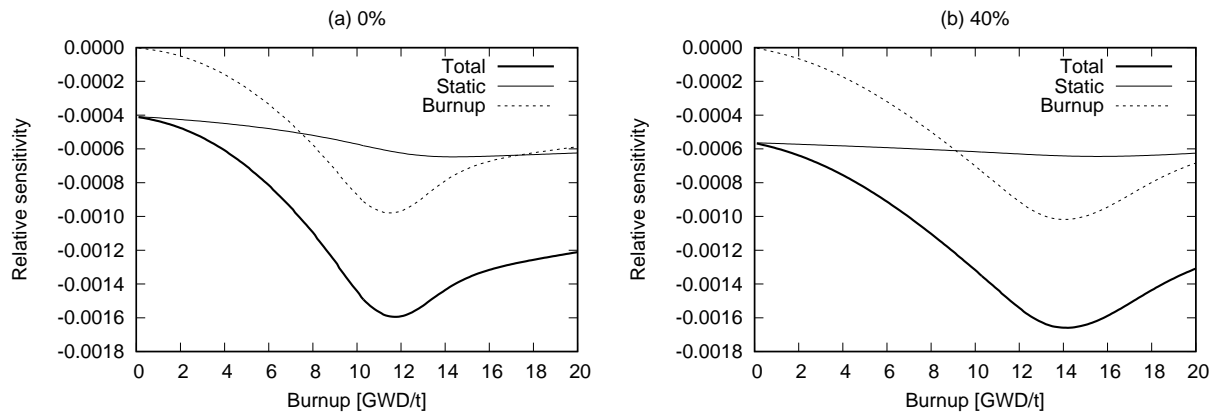


Figure 6: Sensitivity of k to one-group (n, γ) cross sections of gadolinium-154 during nuclear fuel burnup in the 3×3 multicell model

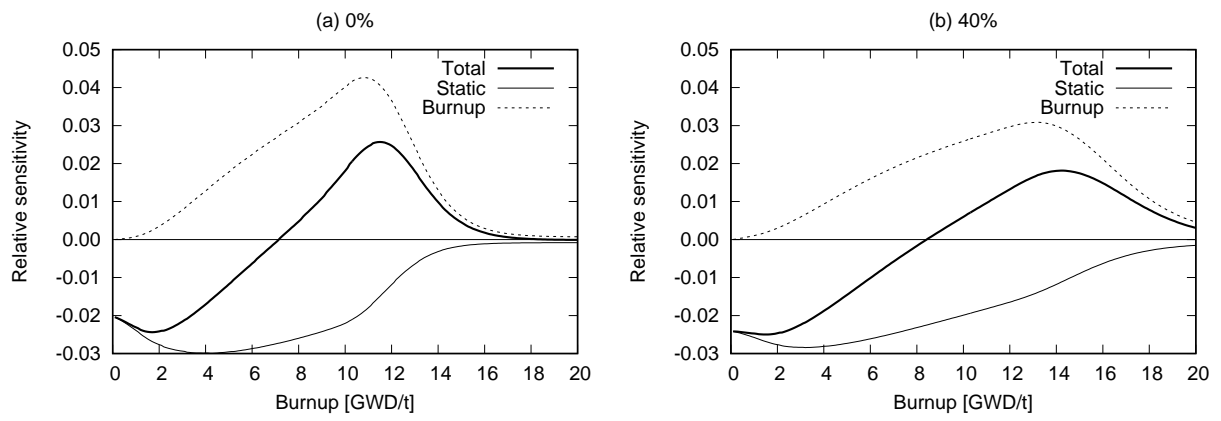


Figure 7: Sensitivity of k to one-group (n, γ) cross sections of gadolinium-155 during nuclear fuel burnup in the 3×3 multicell model

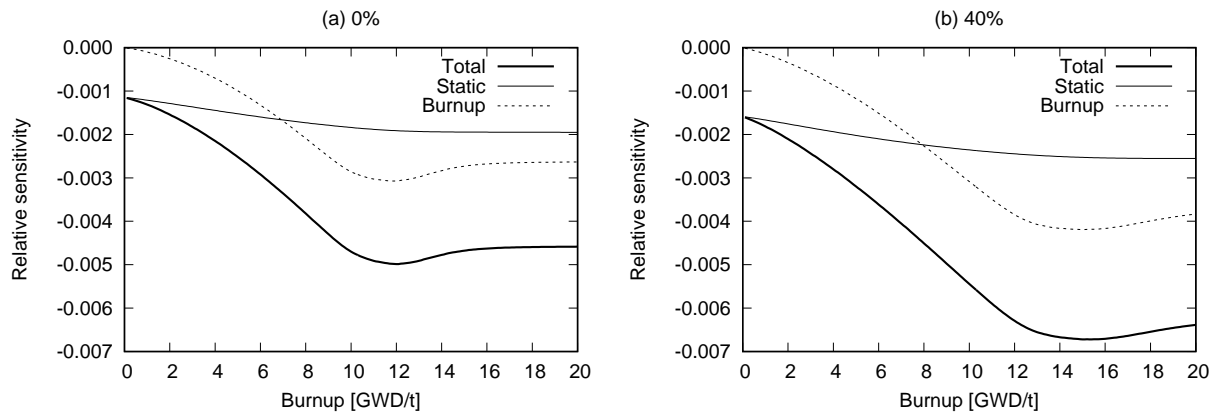


Figure 8: Sensitivity of k to one-group (n, γ) cross sections of gadolinium-156 during nuclear fuel burnup in the 3×3 multicell model

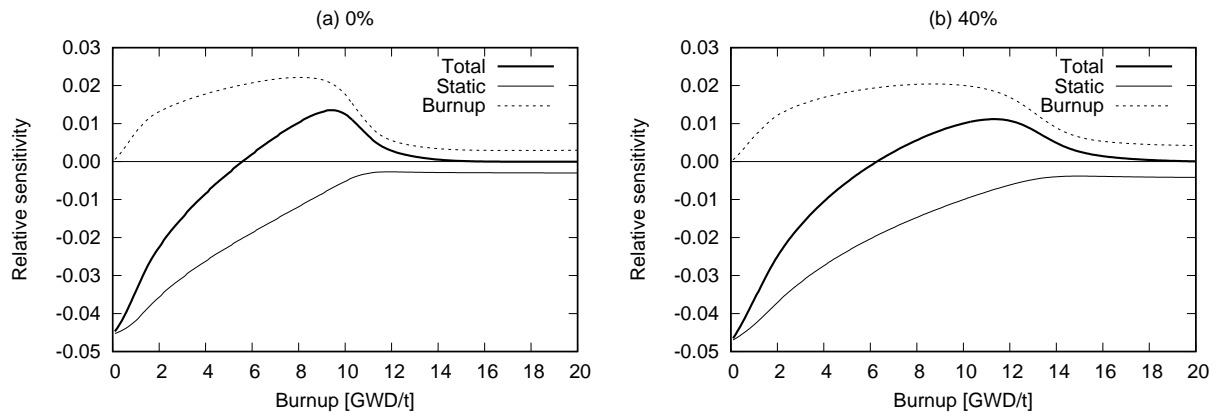


Figure 9: Sensitivity of k to one-group (n, γ) cross sections of gadolinium-157 during nuclear fuel burnup in the 3×3 multicell model

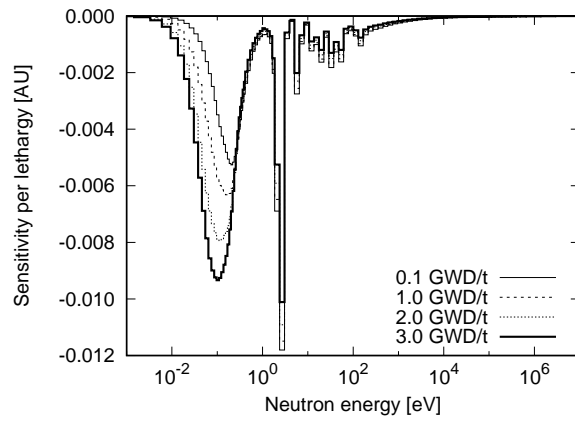


Figure 10: Static component of energy-dependent sensitivity of k to (n,γ) cross sections of gadolinium-155 in the 3×3 multicell model

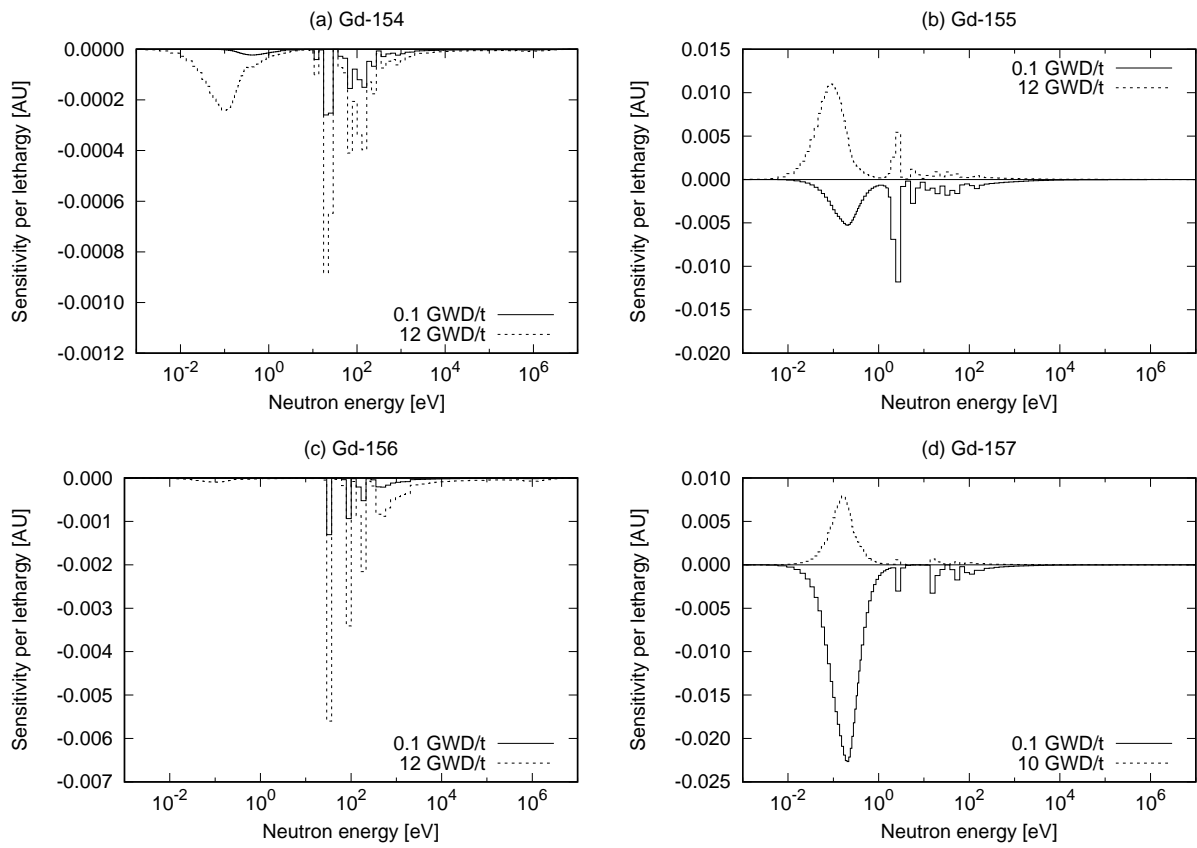


Figure 11: Energy-dependent sensitivity of k to (n,γ) cross sections of gadolinium isotopes in the 3×3 multicell model with 0% void fraction

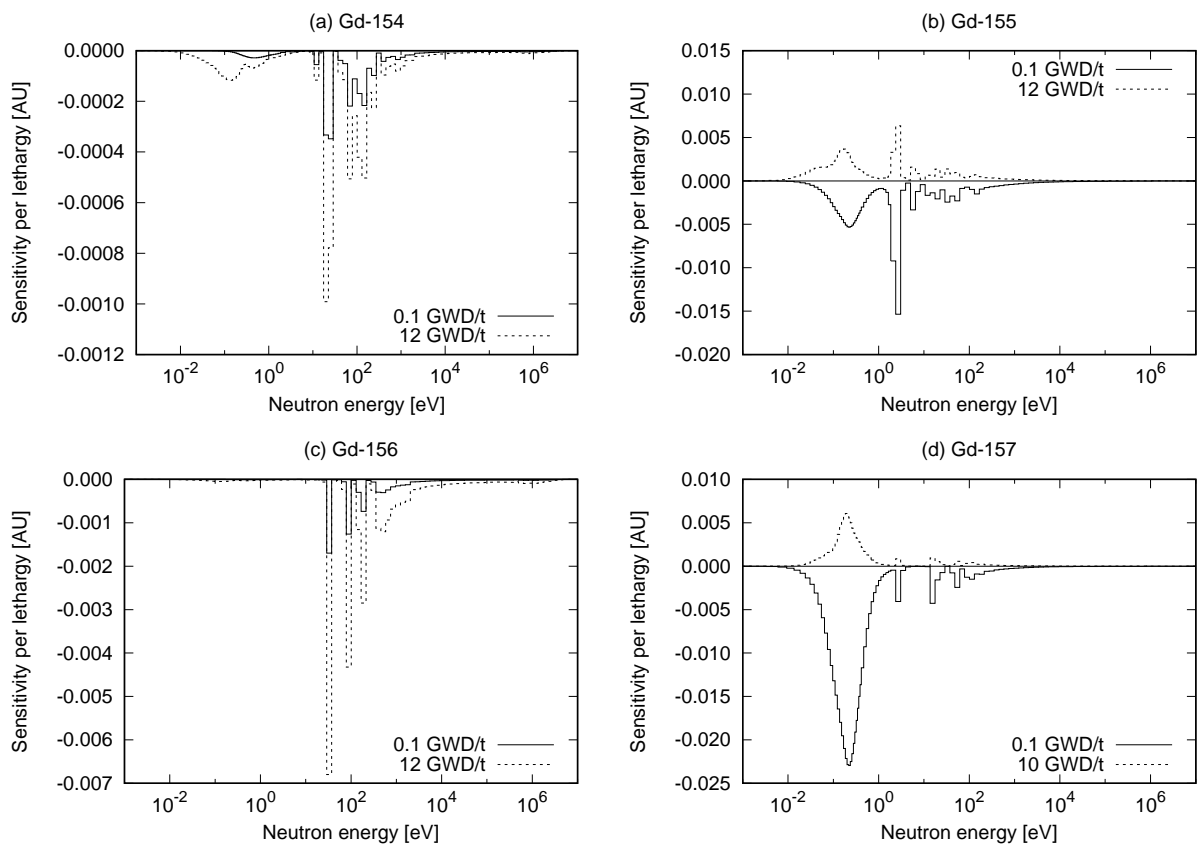


Figure 12: Energy-dependent sensitivity of k to (n, γ) cross sections of gadolinium isotopes in the 3×3 multicell model with 40% void fraction

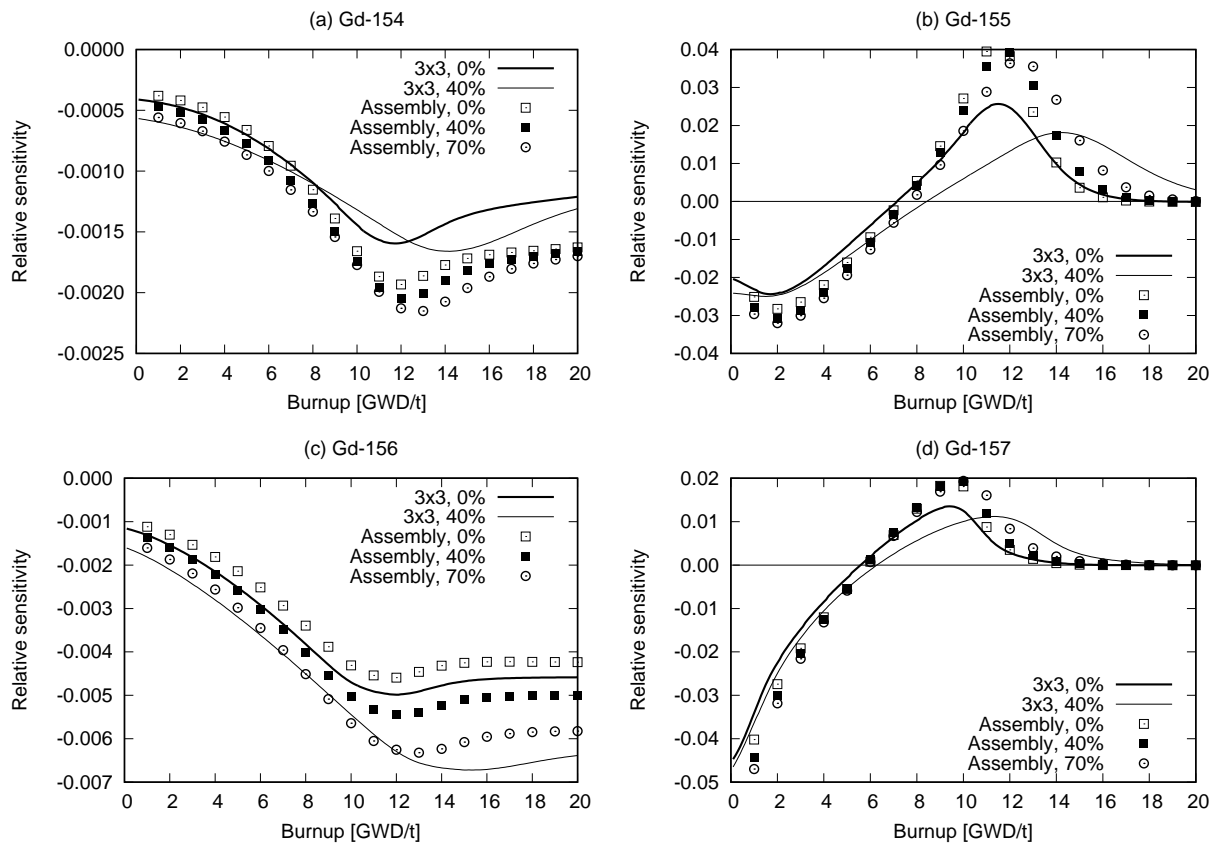


Figure 13: Total sensitivity of k to one-group (n, γ) cross sections of gadolinium isotopes in the BWR assembly

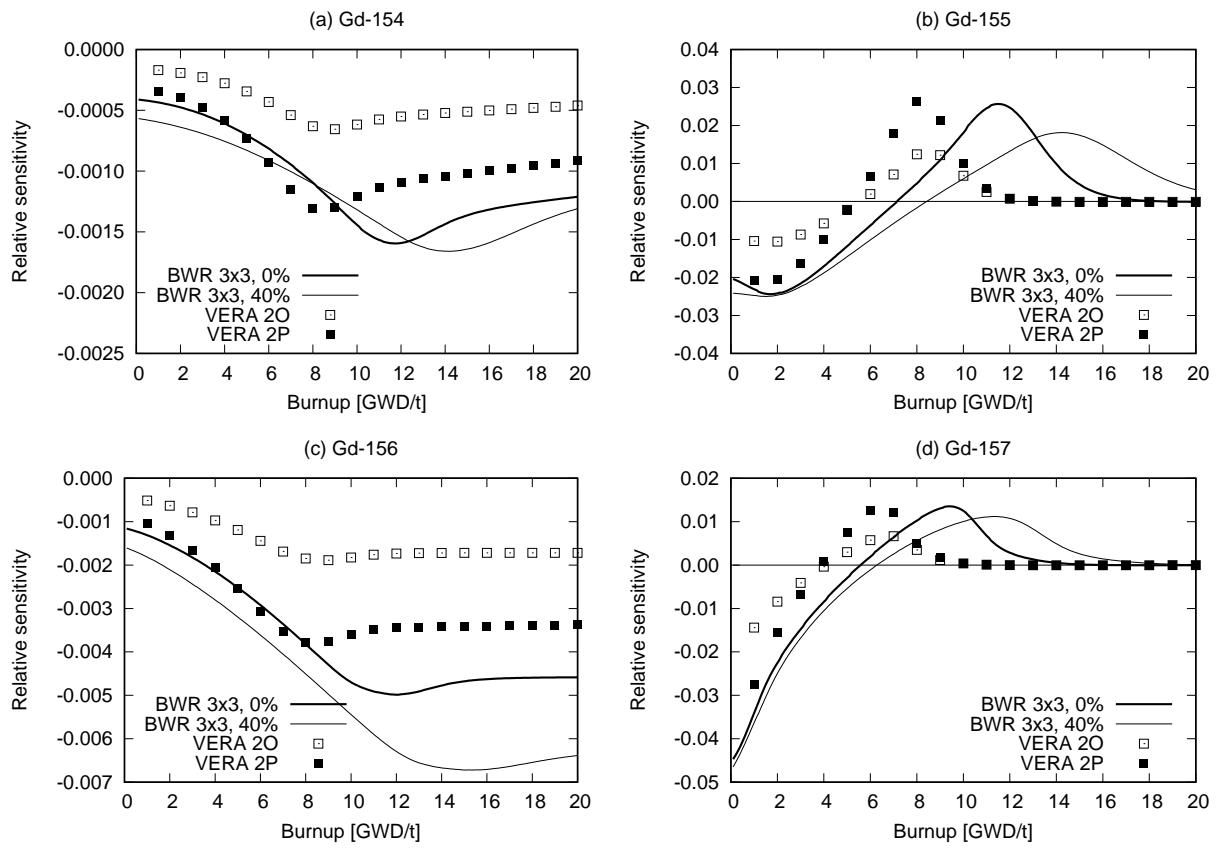


Figure 14: Total sensitivity of k to one-group (n, γ) cross sections of gadolinium isotopes in the PWR assemblies

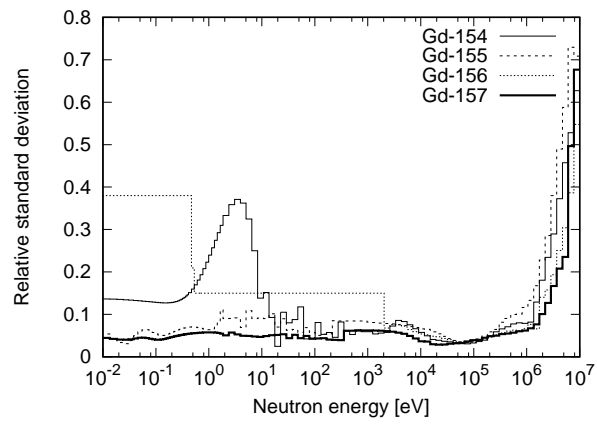


Figure 15: Relative standard deviations of energy group-wise (n,γ) cross sections of gadolinium isotopes

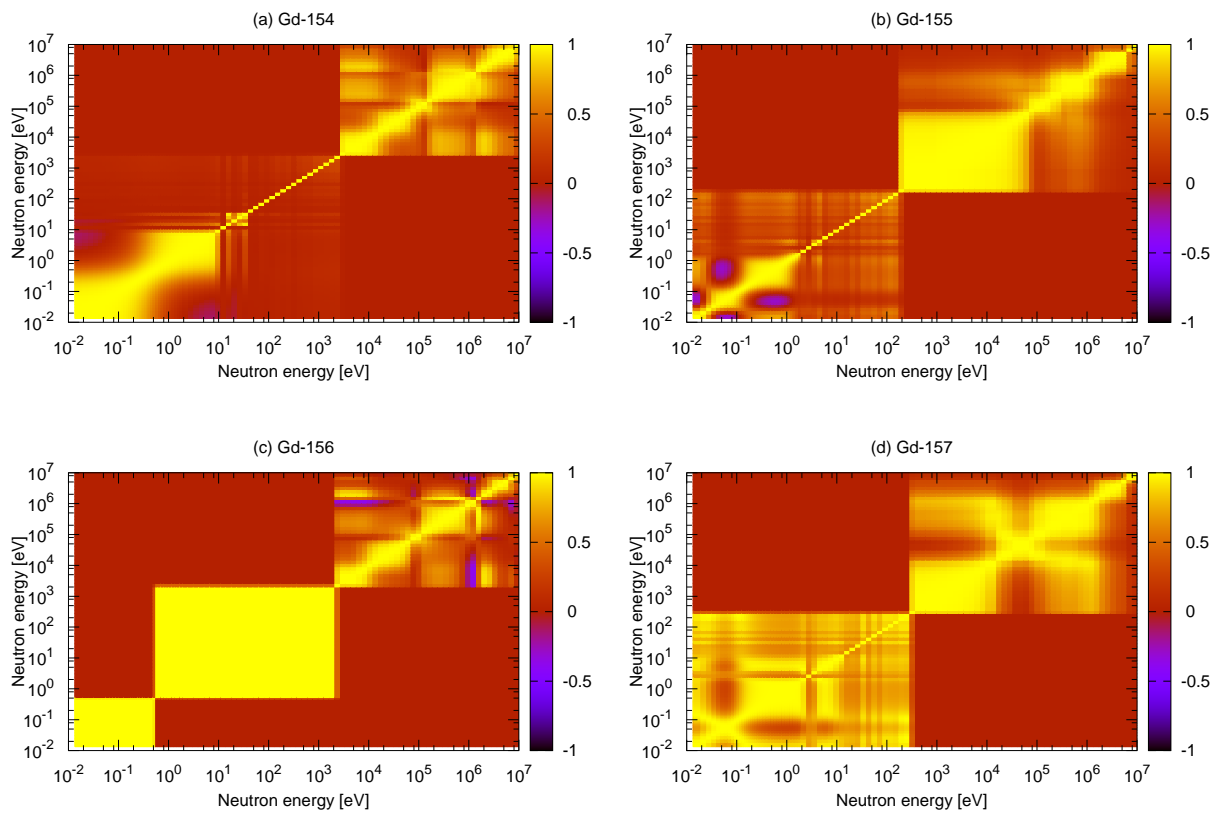


Figure 16: Correlation matrices of energy group-wise (n, γ) cross sections of gadolinium isotopes

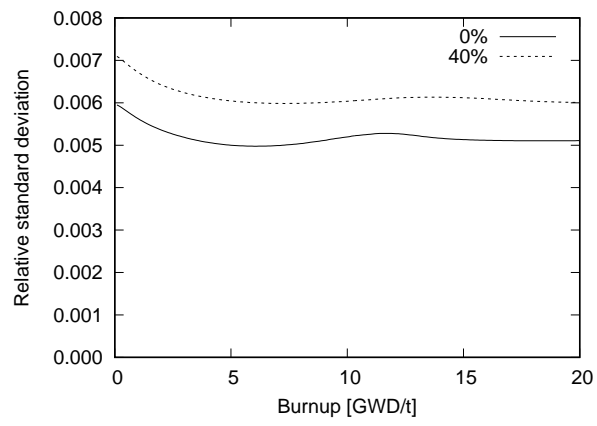


Figure 17: Nuclear data-induced uncertainty of k during nuclear fuel burnup in the 3×3 multicell model

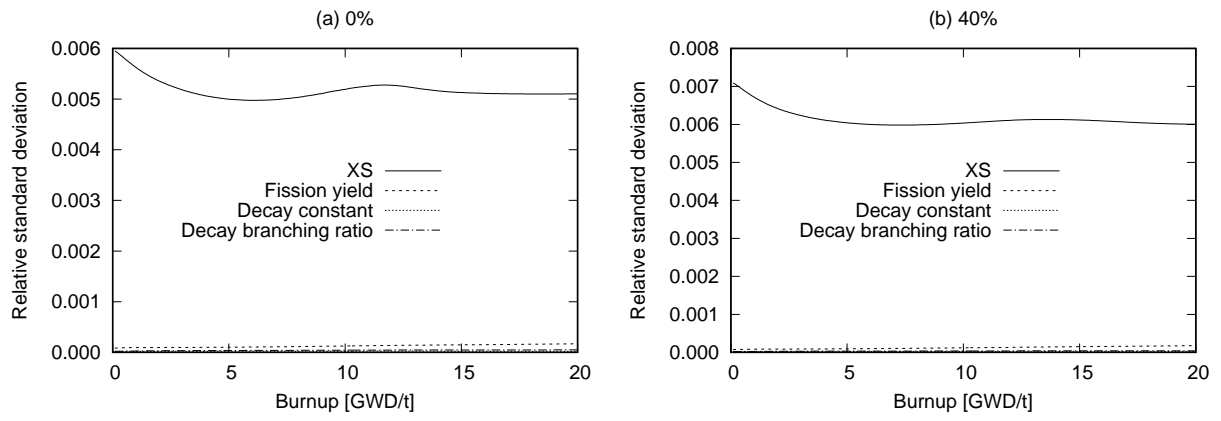


Figure 18: Component-wise nuclear data-induced uncertainty of k during nuclear fuel burnup in the 3×3 multicell model

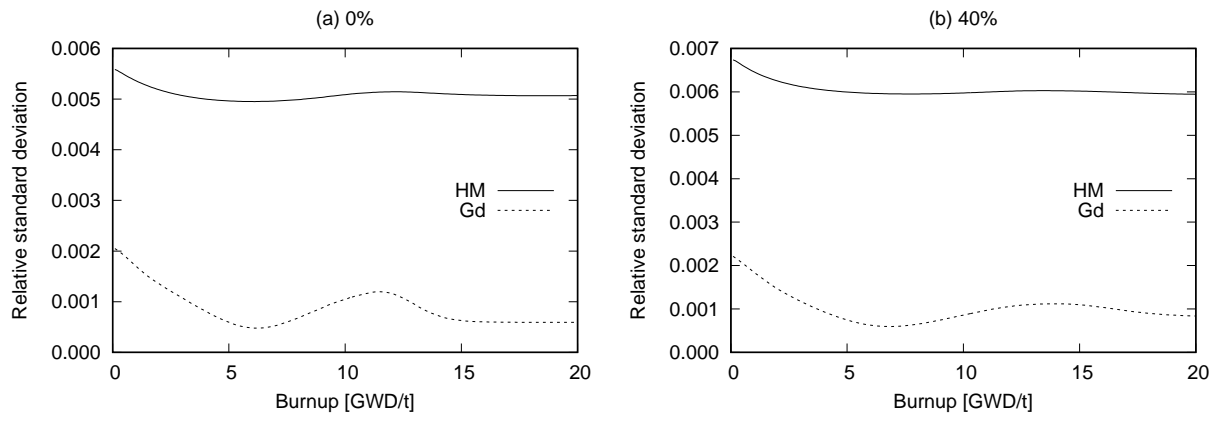


Figure 19: Reaction cross sections-induced uncertainty of k during nuclear fuel burnup in the 3x3 multicell model

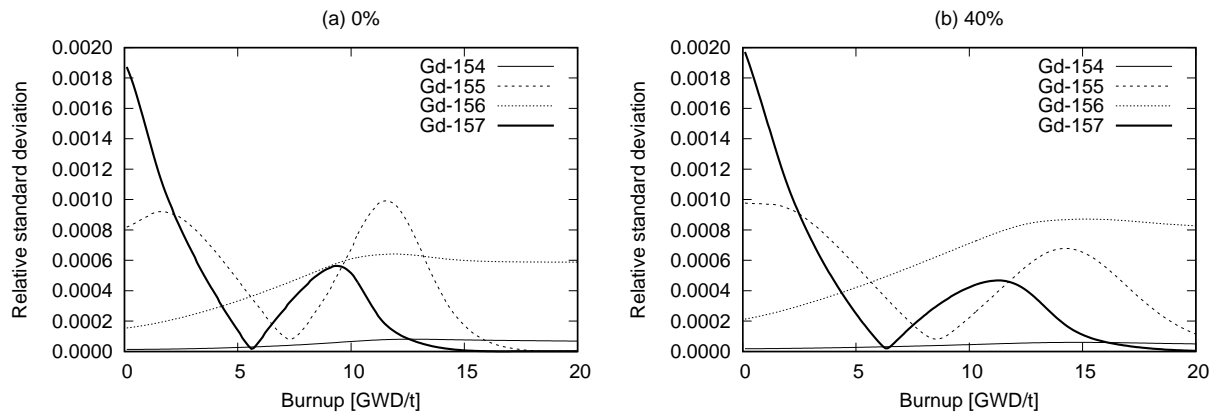


Figure 20: Gadolinium isotope-wise reaction cross sections-induced uncertainty of k during nuclear fuel burnup in the 3×3 multicell model

331 **List of Figure Captions**

332 Fig.1 Geometrical specification of the 3×3 multicell model and the BWR assembly model

333 Fig.2 Infinite neutron multiplication factor of the 3×3 multicell model during nuclear fuel burnup

334 Fig.3 Geometrical specification of the PWR assembly models in the VERA depletion benchmark suite

335 Fig.4 Infinite neutron multiplication factor of the BWR assembly with different void fraction

336 Fig.5 Infinite neutron multiplication factor of the PWR assemblies

337 Fig.6 Sensitivity of k to one-group (n,γ) cross sections of gadolinium-154 during nuclear fuel burnup in the 3×3 multicell model

338 Fig.7 Sensitivity of k to one-group (n,γ) cross sections of gadolinium-155 during nuclear fuel burnup in the 3×3 multicell model

339 Fig.8 Sensitivity of k to one-group (n,γ) cross sections of gadolinium-156 during nuclear fuel burnup in the 3×3 multicell model

340 Fig.9 Sensitivity of k to one-group (n,γ) cross sections of gadolinium-157 during nuclear fuel burnup in the 3×3 multicell model

341 Fig.10 Static component of energy-dependent sensitivity of k to (n,γ) cross sections of gadolinium-155 in the 3×3 multicell model

342 Fig.11 Energy-dependent sensitivity of k to (n,γ) cross sections of gadolinium isotopes in the 3×3 multicell model with 0% void fraction

343 Fig.12 Energy-dependent sensitivity of k to (n,γ) cross sections of gadolinium isotopes in the 3×3 multicell model with 40% void fraction

344 Fig.13 Total sensitivity of k to one-group (n,γ) cross sections of gadolinium isotopes in the BWR assembly

345 Fig.14 Total sensitivity of k to one-group (n,γ) cross sections of gadolinium isotopes in the PWR assemblies

- 346 Fig.15 Relative standard deviations of energy group-wise (n,γ) cross sections of gadolinium isotopes
- 347 Fig.16 Correlation matrices of energy group-wise (n,γ) cross sections of gadolinium isotopes
- 348 Fig.17 Nuclear data-induced uncertainty of k during nuclear fuel burnup in the 3×3 multicell model
- 349 Fig.18 Component-wise nuclear data-induced uncertainty of k during nuclear fuel burnup in the 3×3 multicell model
- 350 Fig.19 Reaction cross sections-induced uncertainty of k during nuclear fuel burnup in the 3×3 multicell model
- 351 Fig.20 Gadolinium isotope-wise reaction cross sections-induced uncertainty of k during nuclear fuel burnup in the 3×3 multicell model